Available online at www.sciencedirect.com
SCIENCE DIRECT®
Wear 258 (2005) 1787–1793
WEAR
www.elsevier.com/locate/wear

Finite element analysis and experiments of metal/metal wear in oscillatory contacts

Nam Ho Kim[a], Dongki Won[a], David Burris[a], Brian Holtkamp[b], Gregory R. Gessel[c], Paul Swanson[c], W Gregory Sawyer[a,*]

[a] *Department of Mechanical and Aerospace Engineering, University of Florida, Gainesville, FL 32611, USA*
[b] *Falex Corporation, Sugar Grove, IL 60554, USA*
[c] *Deere and Company, Moline, IL 61265, USA*

Received 12 July 2004; received in revised form 22 December 2004; accepted 23 December 2004
Available online 20 January 2005

Abstract

A numerical approach that simulates the progressive accumulation of wear in oscillating metal on metal contacts is proposed. The approach uses a reciprocating pin-on-disk tribometer to measure a wear rate for the material pair of interest. This wear rate is an input to a finite element analysis that simulates a block-on-ring experiment. After the simulation, two block-on-ring experiments were performed with the same materials that were studied in the reciprocating pin-on-disk experiments. The results from the finite element analysis were in close agreement with the block-on-ring experimental results. This approach did not either rely on curve fitting or use the block-on-ring experimental data as model inputs. The finite element analyses were performed by progressively changing nodal coordinates to simulate the removal of material that occurs during surface interaction. The continuous wear propagation was discretized and an extrapolation scheme was used to reduce computational costs of this simulation.

Keywords: Wear modeling; Finite element analysis

1. Introduction

It is desirable to design engineering components for infinite life, unfortunately, in systems where parts are in intimate contact and relative motion wear is inevitable such designs are difficult to realize. Wear predictions are typically made using contact pressures and slip calculated from the first wear cycle and do not account for the changes in the geometry during life. Ignoring the coupled evolution of wear and contact conditions has been shown analytically and experimentally to over-predict [1,2] or under-predict life [3,4]. These analytical techniques are limited to two-dimensional steady contacts, and wear is concentrated on only one component (i.e., one part is assumed to be sacrificial), although, analytically Blanchet [1] did allow for wear to occur on both specimens in the model of the 'scotch-yoke'.

Computer aided engineering software is widely used to calculate stresses, fatigue life, modal analysis, stiffness and compliance of a structure; the fatigue life of a mechanical component; the noise in the passenger compartment; the vibration level; and the safety of a vehicle in a crash. Unfortunately, there does not appear to be a standardized method for including wear within finite element analysis. Finite element analysis has been used in tribology and the study of wear to model the phenomena at two widely different length scales. At the microscopic level, models of differential elements are used to study wear mechanisms [5,6]. Macroscopic modeling uses wear rates or other models of wear as inputs to finite element analysis. These numerical experiments then study wear on geometrically simple components [7–9]. This paper focuses on the macroscopic wear process and predicts the worn

* Corresponding author. Tel.: +1 352 392 8488; fax: +1 352 392 1071.
E-mail address: wgsawyer@ufl.edu (W.G. Sawyer).

0043-1648/$ – see front matter © 2004 Published by Elsevier B.V.
doi:10.1016/j.wear.2004.12.014

shape of an oscillating block-on-ring experiment using finite element analysis with all tribological inputs coming from experiments run on a reciprocating pin-on-disk tribometer.

Macroscopic wear modelingwas performed by Podra and Andersson [10] who used an elastic foundation model to calculate the contact pressure distribution and updated the contact surface according to a wear rule. They neglected the shear effect of deformationwhich made it difficult to match both the contact area and maximum contact pressure [11]. They further improved the numerical wear simulation using axisymmetric finite element analysis [7,8]. The contact pressure was calculated from the static finite element analysis and the sliding distance was calculated from the rotational speed. To reduce the total number of simulations, Oqvist [9] applied a variable step size in a two-dimensional wear simulation and compared the results with experimental measurements. The agreement between simulation and experiment was good because the wear coefficient was obtained from the same experiment. Recently, Molinari et al. [5] presented a generalized Archard model by allowing the hardness of the soft material to be a function of temperature. Due to the complexity of the wear model, they only applied to a simple contact problem on the flat surface.

The purpose of the work reported here is to identify critical material wear factors in the oscillating metal-on-metal wear problem, measure these parameters using a simple and inexpensive reciprocating flat geometry wear test and to use these measurements coupled with finite element analysis to predict the wear profile of an experiment with a different wear geometry. The present application is challenging due to the oscillatory sliding motion. After obtaining the wear rate from the reciprocating pin-on-disk experiments, a series of finite element analyses are performed by progressively removing material; this is achieved by moving nodes on the interface in the normal direction. The continuous wear process is discretized into a finite number of steps and the wear rules are applied at each discrete step, requiring an integration scheme. An explicit Euler integration method is employed to numerically integrate the continuous wear progress at discrete steps.

The composition of the manuscript is as follows. First wear rates are obtained from the specimen-level wear test described in Section 2. Second, finite element modeling and simulation results are presented in Section 3. Third, validation of the finite element results is performed in Section 4 using data from block-on-ring experiments. Finally, some concluding remarks and discussion on future directions of research in this area are offered.

2. Experimental method and results for determination of a wear rate

Pin-on-disk tests are performed on the tribometer depicted in Fig. 1 in order to measure the wear rates of the steel samples that were 4340 steel with a surface hardness of 42–58 HRc and RMS surface roughness of 63 nm. An electro-pneumatic

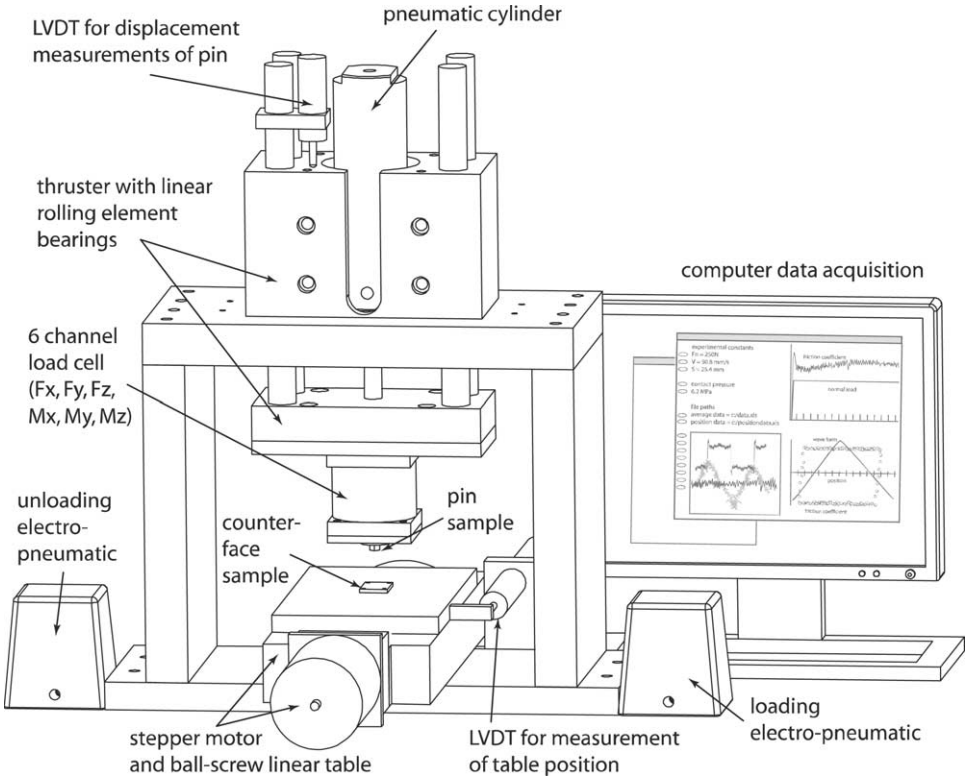

Fig. 1. Schematic of the reciprocating tribometer used to evaluate the wear rate of the self-mated steel contacts. The friction coefficient is continuously monitored and gravimetric analysis of the samples is performed to calculate wear rate.

valve and pneumatic cylinder apply a load of 150 N through a linear thruster that has a six-channel load cell (*Fx*, *Fy*, *Fz*, *Mx*, *My*, *Mz*) mounted at the base. The 6.35 mm diameter steel pin is rigidly mounted to the load cell that outputs normal and friction force voltages to a data acquisition card. The counterface, which is a ground and sanded rectangular plate, is mounted beneath the pin to a linear table. The table is positioned via a stepper motor/ball screw drive. Sliding amplitudes (mm) of 25.4, 6.35, 3.18 and 1.59 are imposed, with speeds (mm/s) of 43.7, 30.2, 21.1 and 14.5, respectively. While the target speed is 50.8 mm/s because of accelerations at the beginning and end of the reciprocating cycles the average sliding speeds are all lower, and with decreasing reciprocating path length the effect becomes more pronounced. For this paper, a dimensionless sliding amplitude is defined as the ratio of sliding amplitude (*S*) to the pin diameter (*D*). This parameter is slightly different than the mutual overlap coefficient introduced by Play [12], which was a ratio of apparent area of contact to the wear track area of the counterface (the mutual overlap coefficient is therefore always between 0 and 1). The masses of both samples are measured before and after each test. The masses of the pins are measured with a precision analytical balance, which has a range of 220 g and a resolution of 10 μg. The disks are too large for the precision analytical balance, so a larger balance with a range of 300 g and a resolution of 1 mg was used for these specimens. The mass loss of theses samples, the density of the material, the total test sliding distance and the time averaged normal load are used to calculate the wear rate with the following equation:

$$K\,(\mathrm{mm}^3/\mathrm{Nm}) = \frac{\text{Mass loss (mg)}}{\rho\,(\mathrm{mg/mm}^3)\,F\,(\mathrm{N})\,d\,(\mathrm{m})} \quad (1)$$

Fig. 2 shows the results from the reciprocating pin-on-disk tests. The experimental uncertainty in these measurements is represented by the error bars, which were calculated according to the method proposed by Schmitz et al. [13]. The experimental results reveal that the wear rates are a strong function of the nondimensional sliding amplitude (Oqvist made a similar observation in a roller-to-plate contact experiment [9]). The convergence of the wear rates of the pin and the counterface at small nondimensional sliding amplitudes is likely related to the entrapment of debris within the contact. These third bodies offer some velocity accommodation within the contact and are thus likely protective.

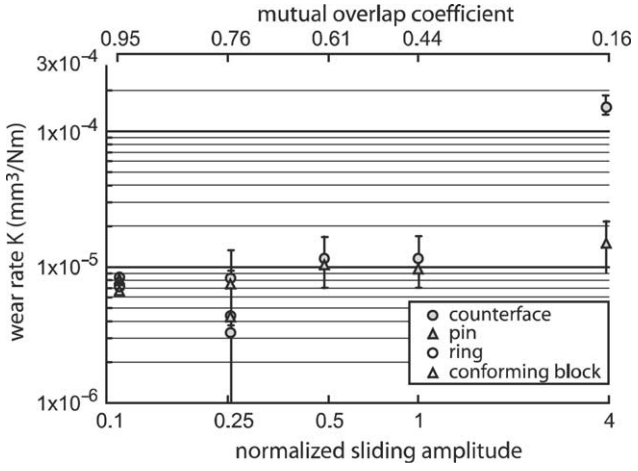

Fig. 2. Wear rate variations as a function of relative sliding amplitude under the same average contact pressure (4.7 MPa) and sliding speed (V = 50.8 mm/s). The data from both the pin-on-disk experiments (filled symbols) and the oscillating block-on-ring experiments (open circles) are plotted.

The goal of this portion of the research effort was to measure a wear rate that would be a reasonable input to the finite element simulation of an oscillating block-on-ring configuration. The particular configuration that was used in the block on ring testing had an oscillation of $\theta = \pm 3^\circ$, which gives a nondimensional sliding amplitude of approximately 0.1. This was below the lowest range that was tested on the reciprocating pin-on-disk tribometer, a wear rate of $K = 1 \times 10^{-5}$ mm^3/(Nm) was selected from the pin on disk experiments shown in Fig. 2; due to the relatively large uncertainty interval associated with this data the nearest overlapping power of 10 was selected for a wear rate.

After the wear rate was selected from reciprocating pin-on-disk experiments, the finite element simulations and the oscillating block on ring experiments were performed independently. On the left-hand side of the graph in Fig. 2 the experimental data from the oscillating block on ring experiments are plotted. It is encouraging to note how well the reciprocating pin-on-disk tests predicted the wear rates from the block-on-ring experiments.

3. Finite element modeling and simulation

The strength of finite element analysis in making wear predictions is its ability to accurately consider both the variation of the contact pressure and the progressive change of the surface geometry caused by material removal in complex three-dimensional components. Thus, it is very important to identify when and how much material should be removed from the models. There are several examples of researchers using finite element analysis to simulate wear [5–8,14] and the basic approach is to: (1) identify the important parameters affecting the material removal rates, (2) determine appropriate wear rates from specimen-level tests, and (3) perform iterative finite element analyses to progressively remove materials during simulation. In this section, the wear rate that is obtained from the reciprocating pin-on-disk testing is used to perform a series of finite element analyses and to estimate the profile of the worn surface.

3.1. Finite element procedure

For finite element modeling and analysis a commercial program, ANSYS, is used to solve the contact problem and

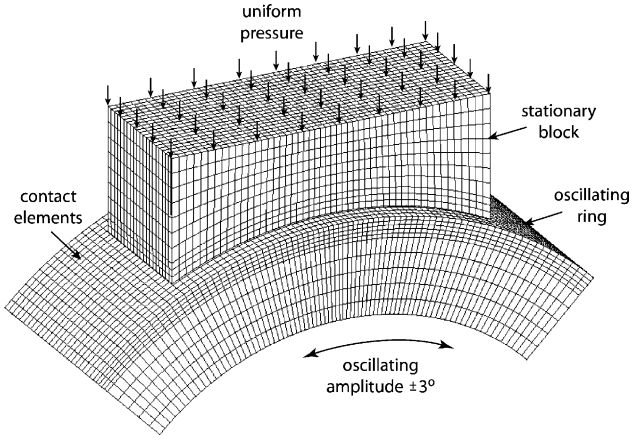

Fig. 3. Schematic of the finite element model for block-on-ring simulation. The load is applied vertically through a uniform pressure that acts normal to the back surface of the block specimen.

to remove materials according to Eq. (2),

$$\frac{\mathrm{d}h}{\mathrm{d}S} = KP \tag{2}$$

where h is the depth of recession of the material normal to the surface, S is the slip distance, K is the wear rate, and P is the surface normal pressure. Although the block geometry is simplified, care is taken to ensure smooth contact pressure variations (see Fig. 3) by dividing the contact surface into a 50×20 finite element mesh. The block and ring bodies and contact surfaces are modeled using 20-node solid elements and 8-node surface elements, respectively. A full quarter of the ring is modeled in order to accommodate the full range of oscillation; the displacement of the ring is fixed at both ends. Uniform contact pressure is applied to the top surface of the block and four low-stiffness rods are attached at the corners of the top surface of the block to remove rigid body motions.

A surface-to-surface contact modeling technique that prevents contact elements (CONTA174) and target elements (TARGE170) from penetrating each other is used. In this contact–target strategy the contact pressure is only calculated for nodes on the contact elements. In order to calculate the wear depth on both surfaces, symmetric contact is used.

To find the contact point locations and pressure an augmented Lagrangian formulation was used. This technique possesses the stability of the penalty method but imposes the impenetrability of the Lagrange multiplier method. The contact problem becomes nonlinear even if the structure experiences a small deformation; thus, the structural equilibrium configuration is found by incrementally changing the applied load. In general, six or seven Newton–Raphson iterations are required to find the converged configuration for each load step.

3.2. Calculations of wear depth and extrapolation techniques

A sequence of computational simulations is performed by rotating the ring by an incremental angle, $\Delta\theta$. Using Eq. (2) the wear depth is then calculated at each incremental angle and material is removed from the model. In general, material wear occurs very slowly and in the finite element analysis of wear, the computational time is of great concern. Since the simulation is performed incrementally, it is practically impossible for currently available computational resources to model every cycle. Thus, an extrapolation scheme must be employed in finite element-based wear simulation. Whenever an interpolation or extrapolation is introduced in the numerical scheme, accuracy and stability become the most important considerations. The errors associated with extrapolation were briefly discussed in Dickrell et al. [4].

In this study three nested approximation/extrapolation schemes are used. First, each oscillation cycle is discretized into 10 steps—five forward and five back. Second, each finite element analysis cycle is assumed to be constant over the next 750 cycles (see [4] for a discussion). Finally, after 40 analysis cycles, which represents 30,0000 experimental cycles, the wear depths are linearly extrapolated to 300,000 cycles (the assumption is that a steady progression of wear is now reasonable). The amount of error introduced by these extrapolations is a function of element size, elastic deformation amount, and incremental wear depth. At this point there is no systematic method to assess this error and it remains an open research topic.

3.3. Updating the finite element models and the contact surfaces

The forward Euler method is used to integrate Eq. (2), and after 1 simulation cycle the result is multiplied by a factor of 750. The wear depth is then updated as shown in Eq. (3).

$$h_j = h_{j-1} + \Delta h_j \tag{3}$$

In Eq. (3), j is a specific computational cycle and Δh_j is an incremental wear depth at this jth cycle and is calculated at each boundary node. The contact condition is imposed at Gauss–Legendre quadrature points, but the contact pressure is calculated only at corner nodes. The average of the contact pressures at the end nodes becomes the pressure of the mid-side nodes. In addition to the contact pressure, surface normal directions are needed to calculate wear depth. The direction normal to the contact surface can be calculated using element geometry and the interpolation scheme of the finite element. However, at the element edge, the normal directions calculated from adjacent elements are in general different because the finite elements have C^0 continuity (1st order and higher derivatives are discontinuous). The normal direction is approximated by taking the cross-product of the two diagonal vectors. Each node is then repositioned by Δh_j in the

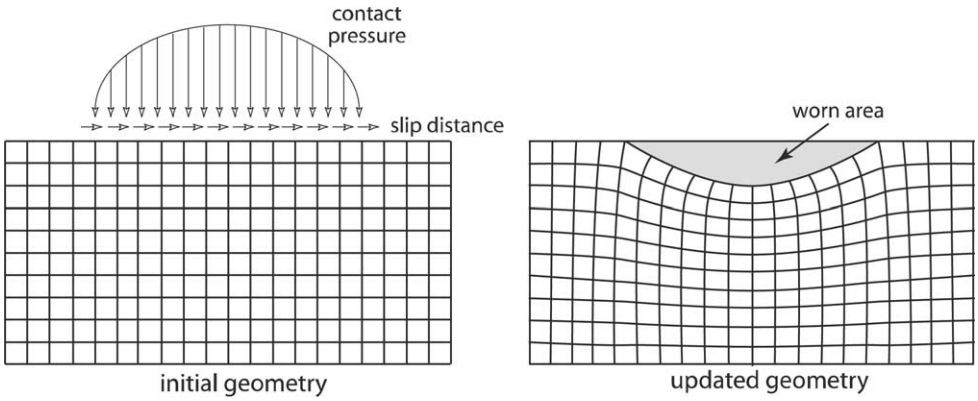

Fig. 4. A schematic of the boundary displacement method used to update the model. Although greatly exaggerated, the schematic illustrates the repositioning of the interior nodes of the finite element model as well as the surface elements.

direction normal to the contact surface. This repositioning of boundary nodes distorts the mesh for those elements in the boundary layer and will eventually ruin element topology. Thus, it is necessary to implement a strategy by which the regularity of the finite element mesh can be maintained. Inspired by a structural shape optimization procedure [15] a boundary displacement method is adopted such that the movement of internal nodes minimizes mesh distortion (see Fig. 4). This method requires the solution of a linear matrix equation.

3.4. Finite element analysis results

Fig. 5 shows the centerline wear profiles of the ring and block that were calculated by the finite element analysis simulation. The ring spans from 0° to 90° and the block spans an angle from 18.25° to 71.73° (the modeled portion of the ring is larger than the block).

The maximum wear depth of the ring is −0.0505 mm, and occurs at the center of contact. The average wear depth is −0.04157 mm. For the block, the maximum wear of −0.07166 mm occurs at either end, and has an average wear depth of −0.05275 mm. Near the center, the wear depth of the block is very close to that of the ring, which is expected because at this location nearly identical contact conditions exist on both parts. Based on the wear profile, it is clear that the radii of the ring and block are increased as a result of wear.

3.5. Analytical predictions of wear depth using initial contact conditions

An analytical estimate of wear depth begins by using linear Hertzian theory [16] of cylinder-to-cylinder contact, with a negative radius of curvature for the block, to calculate the interface contact pressure distribution. The wear depth and profile is then calculated assuming that this contact pressure distribution is constant for all 300,000 cycles. Using a 74.25 N/mm line load, which matches the experimental conditions in Section 4, the Hertzian pressure profile is semi-elliptic with a maximum pressure of 6.04 MPa. Using Eq. (3) and a wear rate of $K = 1.0 \times 10^{-5}$ mm^3/Nm, the wear depth profile after 300,000 cycles can be estimated by multiplying the contact pressure profile by the wear rate and the cumulative sliding distance.

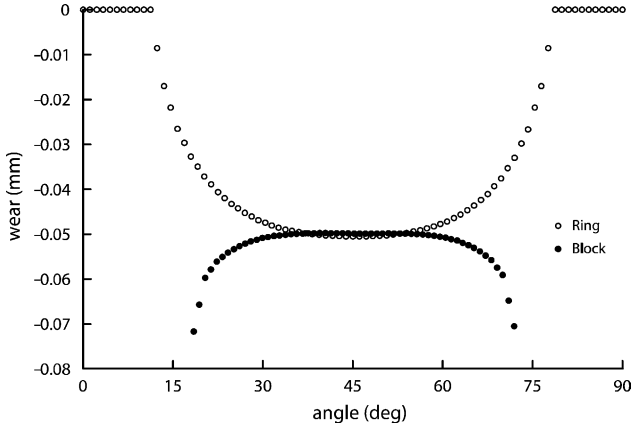

Fig. 5. Wear depth estimated from finite element analyses for the block-on-ring test after 300,000 simulated cycles as a function of the angular coordinate along the ring (45° is the central position).

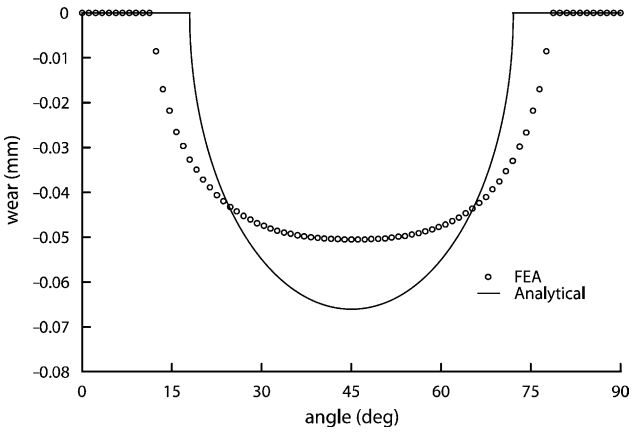

Fig. 6. Wear depth comparison between finite element analyses and an extrapolated analytical solution based on 1st cycle contact pressure.

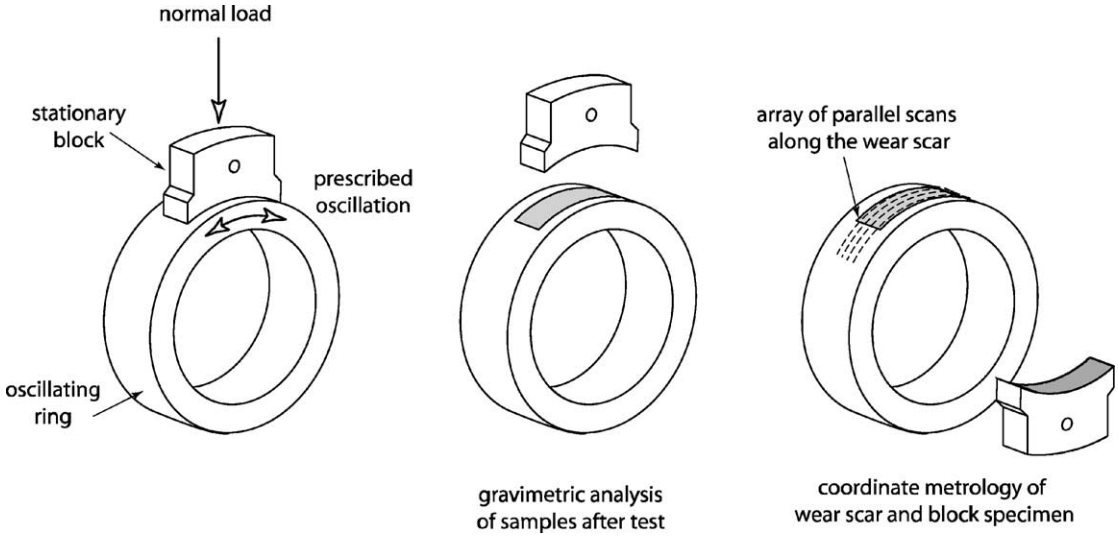

Fig. 7. Schematics of the conforming block-on-ring test and the method of measuring the dimensional changes of the block and ring specimens.

Table 1
Test conditions for the block-on-ring test

Applied force	470 N
Contact area	1 cm^2
Average contact pressure	4.7 MPa
Oscillation angle	$\pm 3^\circ$
Frequency	5 Hz
Test duration	300,000 cycle
Total sliding distance	1098.8 m
Density of materials	7.85 g/cm^3

For the 1098.8 m of sliding distance used in the FEA simulation, the Hertzian wear model estimates a maximum wear depth of $h = -0.066$ mm. The analytical wear profile is compared with the FEA wear profile in Fig. 6. The analytical profile is deeper and narrower than the FEA profile. This is expected since preferential removal of material from areas of high contact pressure and slip will flatten the pressure distribution eventually evenly distributing wear across the contacting surface.

4. Block on ring testing

The block-on-ring test is used to validate the FEA results, which is illustrated in Fig. 7. The ring has a diameter of 35 mm and the projected contact area of the conforming block is100 mm^2. A vertical force is applied to the block, which creates the interfacial pressure profile. The ring is oscillated $\pm 3^\circ$ at 5 Hz. The experimental conditions are given in Table 1. The temperature of the specimen was monitored at 1 Hz and was reported to be stable in the temperature range from 61 to 65 °C. After completing an experiment, the mass loss of each sample was measured using a precision analytical balance, which has a range of 220 g and a resolution of 10 μg. The wear rates from these experiments were calculated using Eq. (1), plotted in Fig. 2 and given in Table 2. The calculated wear rate of 0.8×10^{-5} mm^3/Nm was within the uncertainty interval of a wear-rate obtained from the pin-on-disk experiments although it is about 20% lower than the wear rate used in the simulations, which was $K = 1.0 \times 10^{-5}$ mm^3/Nm. Two samples were run under as nearly identical conditions as possible.

The wear depths of the specimens were measured using a coordinate measurement machine. The tip of the CMM is composed of a sphere with diameter of 1 mm. Multiple scans across the worn surface were made and the initial curvature of the surfaces was subtracted, this is shown in Fig. 8 for both samples together with the finite element predictions. A maximum wear value of -0.057 mm occurs near the center of the wear profile for both specimens.

5. Discussion and concluding remarks

These results from the block on ring experiments and the finite element simulation are close, supporting the possibility

Table 2
Conforming block-on-ring test results (300,000 cycles, 4.7 MPa contact pressure, 1 cm^2 contact area, 5 Hz speed, 1098.8 m sliding distance)

Test	Block			Ring		
	Mass loss (g)	Depth (mm)	Wear rate (mm^3/Nm)	Mass loss (g)	Depth (mm)	Wear rate (mm^3/Nm)
1	0.0324	0.04127	0.80E-5	0.0343	0.03915	0.76E-5
2	0.0334	0.04255	0.82E-5	0.0341	0.03892	0.75E-5
FEA	0.0414	0.05275	1.00E-5[a]	0.0364	0.04157	1.00E-5[*]

[a] Wear rate is an input to FEA. It comes from pin-on-disk tests, not block-on-ring experiments.

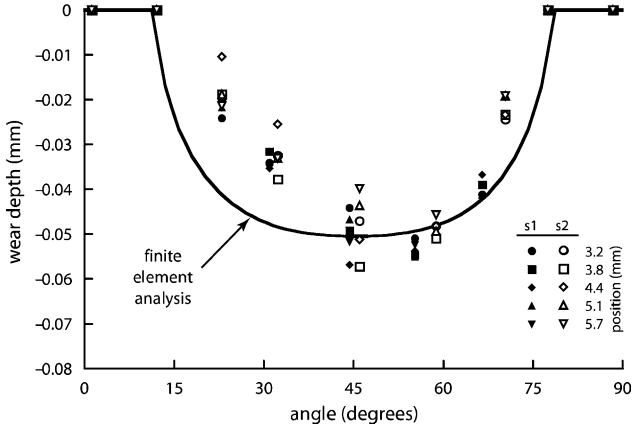

Fig. 8. Comparisons between the finite element analysis and the measured dimensional changes of the block-on-ring experiments of the oscillating ring specimen.

of using finite element analysis coupled with specimen-level test data to estimate wear.

A systematic approach to numerical modeling, simulation, and validation for metal-on-metal wear is developed using both experimental and computational tools. Maximum wear depth predictions produced by finite element simulation of the block-on-ring test agree to within 88% of the experimental measurements without using curve fitting. Computer simulation of the wear process requires an extrapolation scheme and more research is needed in order to systematically identify appropriate extrapolation size as a function of test conditions.

Acknowledgement

This research was supported in part by John Deere - ADV and this support is gratefully acknowledged.

References

[1] T.A. Blanchet, The interaction of wear and dynamics of a simple mechanism, J. Tribol. Trans. Asme 119 (1997) 597–599.
[2] W.G. Sawyer, K.I. Diaz, M.A. Hamilton, B. Micklos, Evaluation of a model for the evolution of wear in a scotch-yoke mechanism, J. Tribol. Trans. Asme 125 (2003) 678–681.
[3] W.G. Sawyer, Wear predictions for a simple-cam including the coupled evolution of wear and load((C)), Lubr. Eng. 57 (2001) 31–36.
[4] D.J. Dickrell, D.B. Dooner, W.G. Sawyer, The Evolution of geometry for a wearing circular cam: analytical and computer simulation with comparison to experiment, J. Tribol. Trans. Asme 125 (2003) 187–192.
[5] J.F. Molinari, M. Ortiz, R.A. Radovitzky, E. Repetto, Finite element analysis of dry sliding wear in metals, Eng. Comput.: Int. J. Comput.-Aided Eng. 18 (2001) 592–610.
[6] P. Ireman, A. Klarbring, N. Stromberg, Finite element algorithms for thermoelastic wear problems, Eur. J. Mech. a-Solids 21 (2002) 423–440.
[7] P. Podra, S. Andersson, Finite element analysis wear simulation of a conical spinning contact considering surface topography, Wear 224 (1999) 13–21.
[8] P. Podra, S. Andersson, Simulating sliding wear with finite element method, Tribol. Int. 32 (1999) 71–81.
[9] M. Oqvist, Numerical simulations of mild wear using updated geometry with different step size approaches, Wear 249 (2001) 6–11.
[10] P. Podra, S. Andersson, Wear simulation with the winkler surface model, Wear 207 (1997) 79–85.
[11] Y. Bei, B.J. Fregly, W.G. Sawyer, S.A. Banks, N.H. Kim, The relationship between contact pressure, insert thickness, and mild wear in total knee replacements, Comput. Model. Eng. Sci. 6 (2004) 145–152.
[12] D. Play, Mutual overlap coefficient and wear debris motion in dry oscillating friction and wear tests, Asle Trans. 28 (1985) 527–535.
[13] T.L. Schmitz, J.E. Action, D.L. Burris, J.C. Ziegert, W.G. Sawyer, Wear-rate uncertainty analysis, J. Tribol. 126 (2004) 802–808.
[14] D.H. Kim, Y. Lee, S.J. Yoo, W.Y. Cho, B.M. Kim, Prediction of the wear profile of a roll groove in rod rolling using an incremental form of wear model, in: Proceedings of the Institution of Mechanical Engineers, Part B-J. Eng. Manufact. 217 (2003) 111–126.
[15] K.K. Choi, K.H. Chang, A study of design velocity field computation for shape optimal design, Finite Elem. Anal. Des. 15 (1994) 317–341.
[16] J. Halling, T.L. Whomes, P.B. Davies, R.D. Arnell, Tribology: Principles and Design Applications, Springer Verlag, 1993.